



Cite this: *Analyst*, 2018, **143**, 5918

Received 16th July 2018,  
 Accepted 29th September 2018

DOI: 10.1039/c8an01322e

[rsc.li/analyst](http://rsc.li/analyst)

## Dual purpose fibre – SERS pH sensing and bacterial analysis†

Holly Fleming,<sup>a,b</sup> Sarah McAughtrie,<sup>a,b</sup> Bethany Mills, <sup>b</sup> Michael G. Tanner, <sup>b,c</sup>  
 Angus Marks<sup>a</sup> and Colin J. Campbell <sup>\*a</sup>

The exploitation of fibre based Raman probes has been challenged by often complicated fabrication procedures and difficulties in reproducibility. Here, we have demonstrated a simple and cost-effective approach for sensing pH through an optical fibre, by employing a wax patterned filter paper-based substrate for surface enhanced Raman spectroscopy (SERS). Through this method, high reproducibility between fibres was achieved. In addition to sensing pH, it was possible to extract fluid samples containing *P. aeruginosa* for further analysis. This dual purpose fibre is bronchoscope deployable, and is able to gather information about both the host and pathogen, which may lead to an improved treatment plan in future *in vivo* applications.

## Introduction

With the rising global challenge of antimicrobial resistance, there is an urgent need to reduce unnecessary antimicrobial prescriptions.<sup>1</sup> Ventilator-associated pneumonia (VAP) is the most common infection among the critically unwell in intensive care units (ICUs), with *Pseudomonas aeruginosa* behind many of these infections.<sup>2</sup>

Studies have shown that using the standard methods to identify the infectious agents, often by interpreting non-specific clinical or radiological features combined with culture techniques from sputum samples, was not adequate to diagnose lower tract respiratory infection but required processing of bronchoalveolar lavage fluid (BALF) samples.<sup>3</sup> However, even the use of these samples has a number of limitations. Bacterial cultures typically take up to 3 days for results, but

specifically, these samples can suffer from a lack of sensitivity due to aspirated fluid being prone to contamination from the upper respiratory tract. Molecular sequencing methods such as polymerase chain reactions (PCR) can be overly sensitive, potentially leading to overtreatment of patients. Combined with poor sampling techniques, there is a significant impact on the treatment and management of patients.<sup>4–7</sup>

The correct identification of pathogens causing respiratory infections and the monitoring of their antimicrobial sensitivity is of great importance. In addition to identification, knowing the physiological environment of the site of interest can also hold great value. pH is tightly regulated within cells and their microenvironments, with any deviations from the homeostasis indicating disease processes. Within the lung, an acidic pH can encourage the growth of bacteria, reduce the efficiency of endogenous cationic antimicrobial peptides and inactivate some antibiotics – all factors that contribute to antimicrobial resistance and worsening patient outcome.<sup>8,9</sup>

The need for bed-side based monitoring has driven research efforts with a focus on robust and rapidly responding optical sensor devices. Fibre-based Raman spectroscopy is becoming a popular method for *in vivo* investigations due to its being a non-destructive and minimally invasive technique. Furthermore, it exhibits high spatial resolution and chemical sensitivity, important factors for *in situ* monitoring. However, as Raman scattering is an inherently weak phenomenon, its use for dynamic physiological sensing can be somewhat limited.

Surface enhanced Raman spectroscopy (SERS), where a reporter molecule is adsorbed on to the surface of a metal nanoparticle (NP), can increase the signal intensity by several orders of magnitude over conventional Raman scattering. SERS has been used in many applications, from intracellular physiological sensing, drug delivery sensing, explosive detection and many more.<sup>10,11</sup>

SERS has been demonstrated through fibre previously, however, it has been challenged by difficulties in reproducibility from fibre to fibre, as well as generating SERS signal inten-

<sup>a</sup>EaStCHEM, School of Chemistry, University of Edinburgh, Edinburgh, EH9 3FJ, UK.  
 E-mail: [colin.campbell@ed.ac.uk](mailto:colin.campbell@ed.ac.uk)

<sup>b</sup>Centre for Inflammation Research, Queen's Medical Research Institute, University of Edinburgh, Edinburgh, EH16 4TJ, UK

<sup>c</sup>Scottish Universities Physics Alliance (SUPA), Institute of Photonics and Quantum Science (IPAQS), Heriot-Watt University, Edinburgh EH14 4AS, UK

†Electronic supplementary information (ESI) available. See DOI: 10.1039/c8an01322e



sities great enough to overcome the intrinsic silica fibre background. As a result, much of the focus in this area has been on background suppression through complex fibre designs and correction methods.<sup>12–14</sup>

Paper based substrates for SERS sensing and detection are gaining traction as point-of-care systems due to their low cost and flexible nature.<sup>15–17</sup> One of the difficulties is directing the deposition of NP, due to the inherent wicking ability of filter paper which is both quick and uncontrolled. The use of patterning with a hydrophobic ink can assist with some of these issues, by defining a specified SERS sensing region.<sup>18,19</sup>

Here, we demonstrate a facile and cost-effective SERS substrate capable of ratiometrically measuring pH using SERS, whilst retrieving a biological fluid sample through combining paper and fibre-based systems. The advantages of a wax patterned paper sensing substrate are two-fold, it allows simple controlling of particle deposition and also facilitates an easy way to retrieve biological fluid samples. Our method has been designed to be small enough to be bronchoscope deployable with the ability to reach alveolar regions within the lung, allowing for site specific information to be gathered and so gaining information about both host and pathogen. This approach has also overcome many of the outlined challenges by achieving an easily repeatable fabrication process and generating high signal to noise ratios.

## Results and discussion

### Paper SERS substrate design

The main goal of this research was to provide a simple SERS substrate to combine with a fibre-based approach to sensing, in particular pH. For this purpose, filter paper was chosen as the preferred substrate due to its wide availability and porous nature.

4-Mercaptobenzoic acid functionalised AuNPs (4-MBA; 150 nm,  $3.6 \times 10^8$  particles per  $\mu\text{L}$ ) were pipetted on to filter paper substrates. Repeated depositions of a low volume of AuNPs (2  $\mu\text{L}$  droplets) were applied, to a final volume of 2–8  $\mu\text{L}$ , with drying stages in between, to avoid a loss of AuNPs through soaking and washing through the paper. The size of the spots that contain AuNPs was defined by the volume of the solution, however there is much variance in shape and the spread, or wicking, of the AuNPs within the spots (Fig. 1A, I).

In an effort to overcome the influence of non-uniform capillary wicking, and therefore the low reproducibility of using a filter paper-based SERS substrate, a hydrophobic wax surround was printed onto the filter paper. Solid wax printing is a simple, inexpensive, and quick method, amenable to mass production. Patterning paper with a wax surround allows control of the wicking action of aqueous solutions, confining the dispersion to the hydrophilic areas.<sup>18–20</sup> By limiting the solution containing the AuNPs to a defined area, there is a reduction in variability in AuNP concentration at any point within the hydrophilic area. A substantial difference between applying AuNPs to filter paper with and without a wax barrier

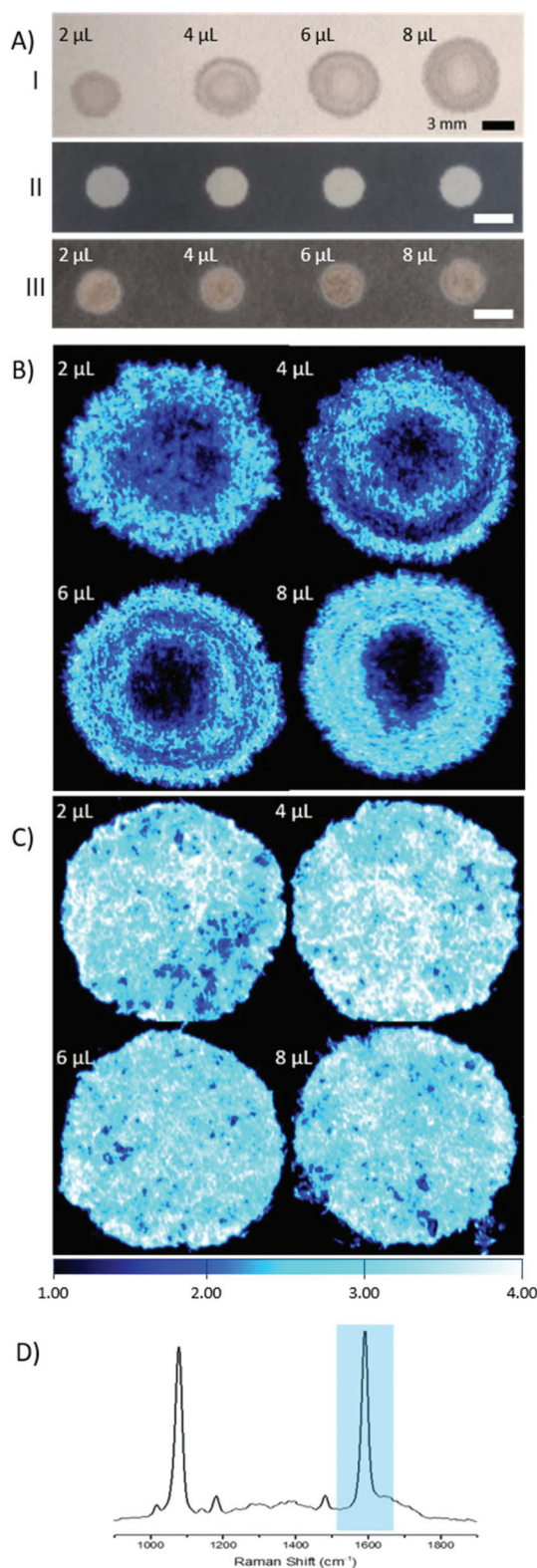


**Fig. 1** Differences between filter paper with waxed boundary and no boundary. (A) I: AuNPs deposited onto filter paper without defined wax boundaries, II: images of filter paper with wax boundary, III: AuNPs deposited onto paper with defined wax boundary. All AuNPs depositions using 2  $\mu\text{L}$  drops. (B) and (C) Raman intensity maps of filter paper and patterned filter paper (respectively), deposited with varying volumes of AuNPs. (D) SERS spectra of 4-MBA, with highlighted peak at  $1587\text{ cm}^{-1}$  used for intensity comparisons.



can be clearly seen by eye (Fig. 1A). The image shows both an increasing spot size, as well as an uneven spread of AuNPs across the filter paper where a wax barrier was not used. The unevenness is further revealed by SERS mapping (Fig. 1B). The patterned paper allows AuNPs to be deposited on the filter paper in a controlled manner, filling the entire hydrophilic area evenly (Fig. 1C). SEM images from paper substrates with a printed wax barrier show a high density of AuNPs on the cellulose fibres, which may help in the formation of SERS “hot-spots”, further enhancing the signal intensity (Fig. S1†).

### Fibre sensing

**Translation to fibre.** While pH sensing using an optical fibre has been demonstrated previously,<sup>12,13</sup> the background Raman scattering from the fibre is strong and can overwhelm the SERS signal from particles deposited on the distal end. Although some of these issues can be alleviated using sophisticated fibre designs, these are often bulky and require multiple fibres or fibres with large bores.<sup>12,21,22</sup> Additionally, many

fibres for use with SERS sensing are prepared by dipping the distal end into concentrated nanoparticle solutions, leading to unknown and variable concentrations on the fibre tip.<sup>12,13,21,22</sup> This has an impact on how reproducible, and therefore scalable, the production of the fibre sensors can be. Keeping in mind the future translation of fibre-based sensors into clinic, the ideal instrument would consist of a single fibre being bronchoscope deployable, with simple fabrication steps and minimal packaging requirements.

The fabrication of the packaged ferrule end is a simple process (Fig. 2A), whereby a 2 mm wide strip of the wax printed AuNP paper was placed, facing upwards, on a ring-shaped section of rubber. The ferrule was pushed through the ring with the paper flush across the top surface. A commercially available 200  $\mu\text{m}$  single core (NA 0.39), multi-mode fibre was then threaded through the ferrule until abutted against the paper, and secured in place at the base of the ferrule.

Through combining the fibre with the paper-based SERS substrate, a controlled particle deposition is achieved, provid-

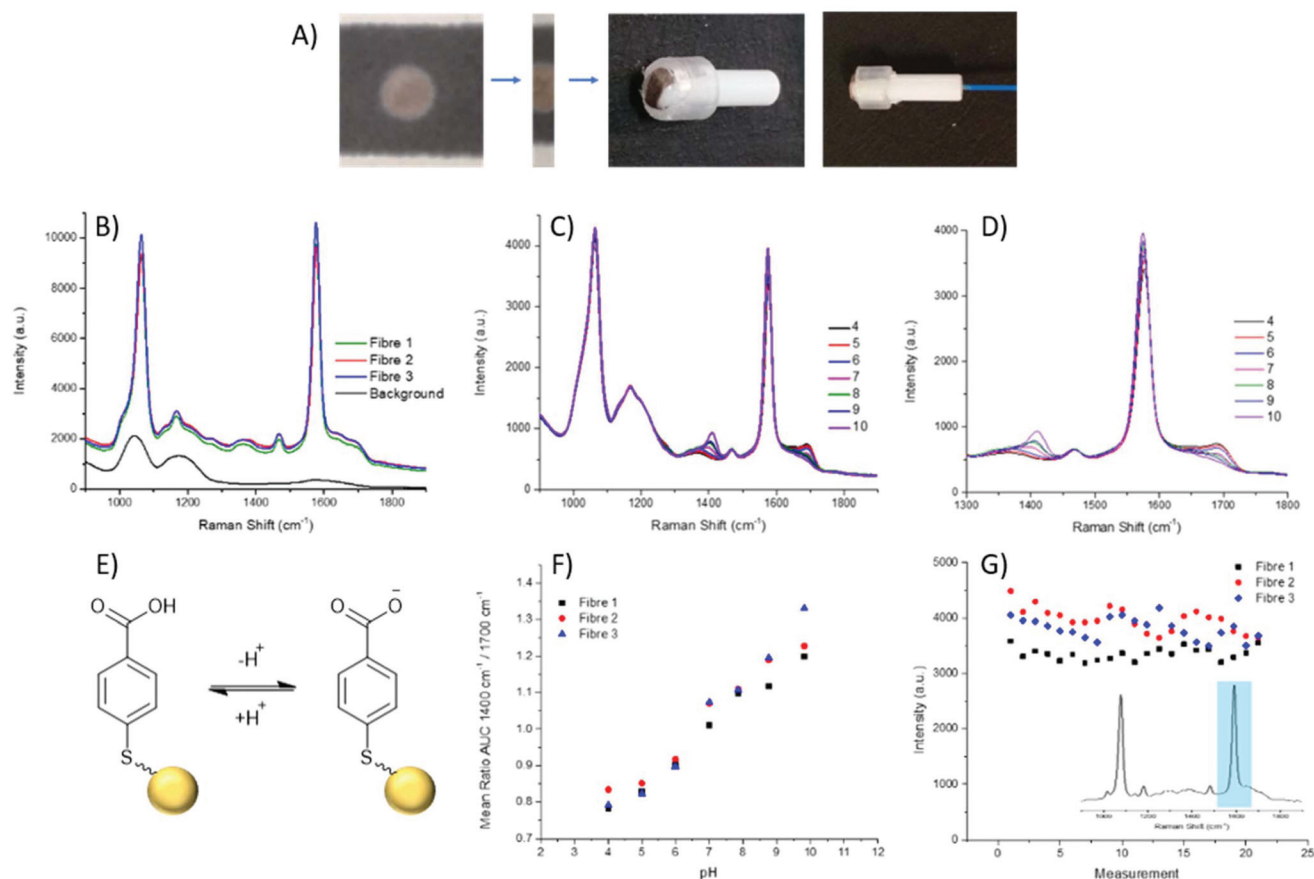


**Fig. 2** (A) Process of fabrication to combine paper SERS substrate with 200  $\mu\text{m}$  core optical fibre. Centre strip of AuNP paper cut and secured across a fibre ferrule, fibre threaded through and secured in place. (B) SERS spectra from 3 separate fibres, displaying similar signal intensities. Black spectrum represents intrinsic fibre background (which is easily overcome by SERS signals), 785 nm, 1 mW, 1 s integration time. (C) SERS spectra of 4-MBA, through fibre, over pH 4–10; (D) shows zoomed range of peaks of interest at 1380  $\text{cm}^{-1}$  and 1700  $\text{cm}^{-1}$  changing over pH 4–10. (E) NP-MBA nanosensors, equilibrium between MBA and its deprotonated form attached to a gold NP (yellow sphere, not to scale). (F) Ratio of Area under Curve (AUC) between 1380  $\text{cm}^{-1}$  and 1700  $\text{cm}^{-1}$  plotted against pH over 3 fibres. Each measurement was taken using 785 nm, 1 mW, 10 s integration time. (G) Intensity of 1587  $\text{cm}^{-1}$  reference peak (inset) obtained during each measurement of the pH calibration plotted in chronological order.





ing confidence that the same signal intensity can be reached in any location where the fibre tip is placed on the AuNP paper. This extends to being able to reliably reproduce a strong signal when moving between fibres. Three separate fibres with packaged distal ends were prepared and their spectra recorded in air. It can be seen that across the three fibres reproducibility of the paper-based system is demonstrated by strong signals of similar intensities (Fig. 2B). Moreover, the strong signal intensity generated by the paper-based SERS sensor easily overcomes the intrinsic fibre background using relatively low laser power and integration time (1 mW and 1 s respectively). Importantly, the fibre background does not impose significantly on the pH sensitive peaks at  $1380\text{ cm}^{-1}$  and  $1700\text{ cm}^{-1}$ .

**pH sensing.** The reporter molecule, 4-MBA, has long been known as sensitive to environmental pH variations, and has been previously demonstrated as a suitable choice for biologically and clinically relevant pH sensing.<sup>11,12,23,24</sup> The peaks observed at  $1380\text{ cm}^{-1}$  and  $1700\text{ cm}^{-1}$  are spectral features most dependent on pH. Under basic conditions (pH 9 and above), 4-MBA is known to be in the anionic form, affording a strong response in the  $1380\text{ cm}^{-1}$  peak. Conversely, under acidic conditions (pH 5 and below), 4-MBA is mostly in the neutral form, generating a clear response in the peak found at  $1700\text{ cm}^{-1}$ .

Aqueous pH buffers were prepared from pH 4–10 and verified with an electrochemical pH meter (Mettler-Toledo). The packaged distal end of the fibre was submerged in buffer and the spectrum recorded after 10 s. Between readings the AuNP-paper substrate was rinsed in  $\text{dH}_2\text{O}$  and blotted dry. Each fibre had three replicate calibrations where pHs were recorded in a random order. Three fibres in total were measured. The spectra were analysed by first normalising the spectra to the magnitude of a reference peak ( $1070\text{ cm}^{-1}$ ), followed by evaluating the area under the curve (AUC) within a  $\pm 25\text{ cm}^{-1}$  window of the peaks at  $1380\text{ cm}^{-1}$  and  $1700\text{ cm}^{-1}$ . Plotting pH against the AUC ratio, all fibres demonstrated consistent variation within the physiological range (Fig. 2F), again indicating the suitability of the paper SERS substrate for fibre sensing in future *in vivo* applications.

The loss of nanoparticles over time from the distal end of the fibre would be problematic, not only due to loss of signal, but also because loss of AuNPs is undesirable for use in *in vivo* applications. With the fibres which have been dip-coated with nanoparticles, typically, a porous sol-gel layer is used to protect the distal end. However, this coating can also suffer from variations in both coating depth and the porosity of the sol-gel layer, which may affect the speed at which measurements can be acquired. The paper SERS substrate showed no significant signal loss from over the course of the pH measurements (approximately 60 min per fibre). The intensity of the  $1587\text{ cm}^{-1}$  peak was plotted over time, with the slight oscillations being attributed to the drying and wetting of the SERS samples. The average intensities between the first and last sets of pH measurements differ by less than 250 counts, less than 10% of overall signal intensity (Fig. 2G).

## Extraction and culture of *P. aeruginosa*

There has been a considerable increase in the number of infections due to antimicrobial resistant bacteria with lower respiratory tract infections responsible for the second highest burden of disease globally.<sup>25–27</sup> Within ICUs, the development of pneumonia is associated with high mortality rates.<sup>28</sup> The investigation of respiratory disease can involve biopsies, an invasive procedure, and the collection of BALF, which can become contaminated by bacteria found in the upper respiratory tract. The ability to sample fluid at specific sites can alleviate issues related to contamination. This fibre has been designed keeping in mind that it should be deployable through a conventional bronchoscope. In this way, it can be extended and retracted at specific region of interest, therefore minimising the contact between the distal end of the probe and upper respiratory tract.

The porous nature of the filter paper not only provides a suitable substrate for the deposition of nanoparticles but also lends itself to retrieving a sample of fluid. We demonstrate that the filter paper is capable of sampling liquid containing bacteria which can then be cultured and counted. A clinical isolate of *P. aeruginosa* 3284 was cultured and prepared for this study.

**Sample retrieval efficiency.** To evaluate whether samples containing bacteria could be retrieved using this method, and to investigate the limit of detection, 10-fold serial dilutions of PA3284 ranging from  $6 \times 10^8$ – $6 \times 10^0$  CFUs (colony forming units) per mL were prepared. The ferrule tip containing the AuNPs soaked paper substrate was dipped in to the bacterial containing solutions and gently pressed into lysogeny broth (LB) agar plates, with three presses per dip. This process was repeated a total of three times per dilution. After an overnight incubation period ( $37^\circ\text{C}$ , 5%  $\text{CO}_2$ ), the colonies were counted and compared to the control (consisting of  $3 \times 20\text{ }\mu\text{L}$  droplets of each dilution) (Fig. 3). We observed a similar number of colonies between the paper and standard methods, with a LOD of 60 CFUs per mL in both the paper-based method and the Miles and Misra method, efficiently detecting below the clinical cut off (above  $10^4$  CFUs per mL to be considered pathogenic).<sup>4,29</sup>

**Direct imaging.** We were able to further extract bacteria from the paper after pressing into agar by placing the paper strip in PBS (500  $\mu\text{L}$ ) and lightly vortexing. Using an in-house ubiquitin based bacterial stain (5  $\mu\text{M}$ ),<sup>30</sup> it was possible to image the live bacteria shortly after retrieval, without the need for a washing step, by confocal laser scanning microscopy (CLSM; Fig. 3B). Using bacteria specific probes enables the *in situ* optical detection of live bacteria in human alveolar lung tissue.<sup>30–32</sup>

In addition, we investigated imaging bacteria directly on the paper itself (Fig. 4). Due to the autofluorescence of the paper (Fig. S2†), a far-red dye was used. The bacteria were labelled with a Syto60 (5  $\mu\text{M}$ ), a fluorescent nuclear stain, before introducing the AuNP-paper strips into the solution containing  $6 \times 10^5$  CFUs per mL. While this strategy sup-



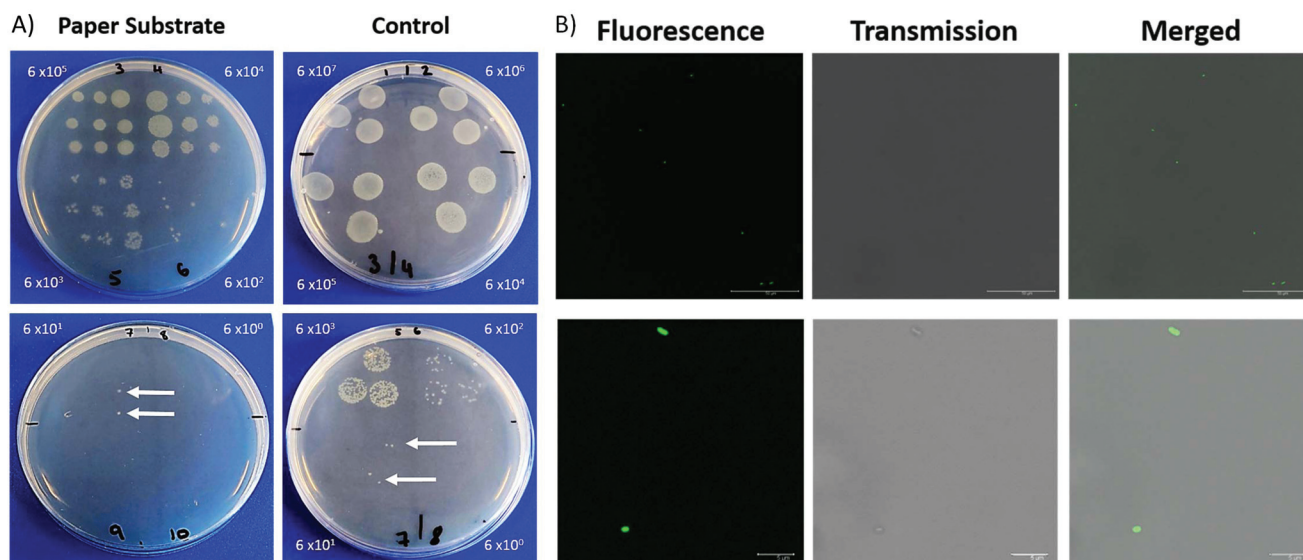


**Fig. 3** (A) *P. aeruginosa* colonies on LB agar. Packaged fibre ferrule dipped into solutions containing ten-fold serial dilutions of bacteria and pressed into plate. Similarly, for the control plates,  $3 \times 20 \mu\text{L}$  droplets pipetted on to the plates. CFUs grown from a concentration above  $6 \times 10^0$  in both the paper ferrule and control samples. White arrows indicate colonies formed at a concentration of  $6 \times 10^1$ . Both conditions incubated overnight at  $37^\circ\text{C}$ ,  $5\% \text{CO}_2$ . Dilutions of *P. aeruginosa* were between, paper substrate:  $6 \times 10^5$ – $6 \times 10^0$  CFU  $\text{mL}^{-1}$ ; control:  $6 \times 10^7$ – $6 \times 10^0$  CFU  $\text{mL}^{-1}$ . (B) Fluorescence images from extracted *P. aeruginosa* in PBS. Ferrule pressed into agar, followed by submerging in PBS, stained with UBI-based dye ( $5 \mu\text{M}$ ).  $6 \times 10^2$  CFU  $\text{mL}^{-1}$  concentration used. Top panel, wide field view, bottom panel, zoom in of *P. aeruginosa*.

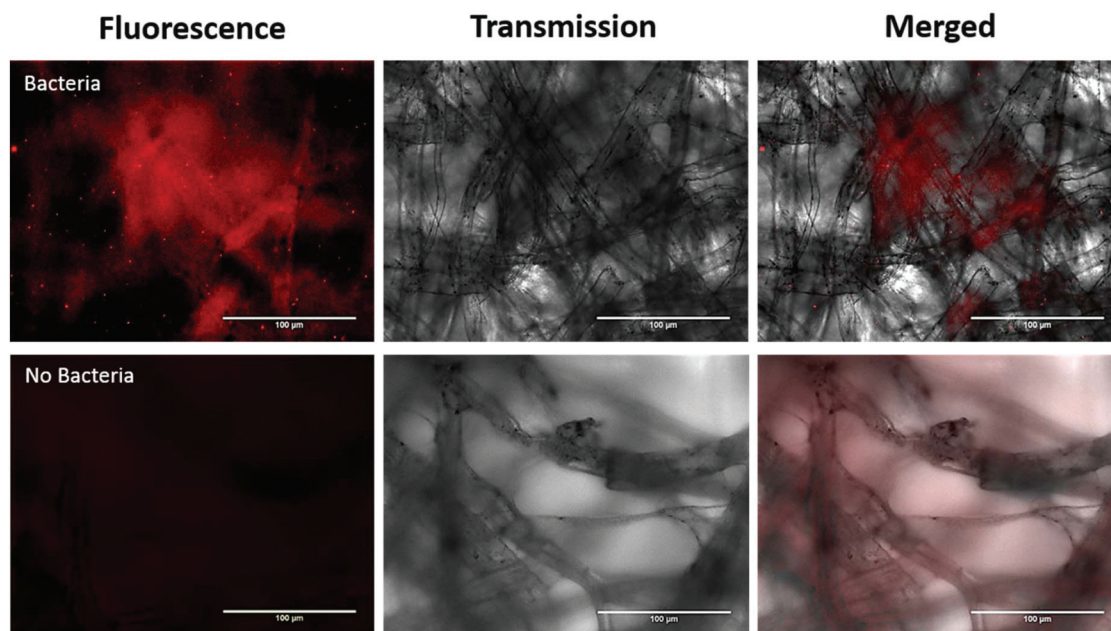


**Fig. 4** Fluorescence images showing bacteria on AuNP-paper substrates. Bacteria were treated with Syto60 ( $5 \mu\text{M}$ ), the top row consists of AuNP-paper containing bacteria, merged, transmission, and fluorescence images. The bottom row corresponds to AuNP-paper without bacteria.

pressed much of the autofluorescence seen in the green channel, there is still some homogeneous signal observed in the Cy5 fluorescence channel. However, despite the background signal, the labelled bacteria can clearly be detected by widefield imaging, indicating that augmenting collected

samples with an appropriate far-red bacteria-specific stain could enable *in vivo* bacterial detection on fibre without any need for a processing step. This could pave the way for simultaneous measurements for bacteria and pH through a single fibre.



## Experimental section

### Materials and reagents

Gold nanoparticles in citrate buffer (AuNPs, 150 nm, put concentration), poly-L-lysine (30 000–70 000 MW), 4-mercaptobenzoic acid (4-MBA) were all purchased from Sigma-Aldrich. Filter paper (Whatman, grade 114) was purchased from Scientific Laboratory Supplies Ltd. Lysogeny Broth was purchased from Thermofisher. Both the optical fibre (200  $\mu$ m core diameter, NA 0.39) and fibre ferrules were purchased from Thorlabs.

### Instrumentation

Solid wax printing was carried out using a Xerox ColourQube8580.

SERS maps were collected on a Renishaw In Via system, using a 785 nm laser, 5 $\times$  objective, at  $\sim$ 1.5 mW laser power with a 1.4 s integration time.

The fibre-based SERS spectra were collected using a home built optical set up specifically for optical fibres.<sup>12</sup> A 785 nm laser line (Thorlabs) was used as the excitation source, coupled to an OceanOpticsPro spectrometer. The output of the laser power was set as 1 mW, and an integration time of 10 s was used.

Images of bacteria extracted from paper fluorescent were taken by confocal laser scanning microscopy (Leica SP8, 488 nm excitation, 63 $\times$  oil immersion). Images were brightness and contrast enhanced with proprietary software. Bacteria imaged directly on waxed AuNP paper were taken using an EVOS<sup>®</sup> microscope with GFP and Cy5 light cubes, images were brightness and contrast enhanced using ImageJ software.

### Methods

**Preparation of functionalised nanoparticles.** Gold nanoparticles (5  $\times$  1 mL aliquots,  $3.6 \times 10^9$  particles per mL,  $\sim$ 150 nm) were prepared for functionalisation by centrifuged at 5500 rpm for 10 min. For functionalising the particles, following centrifugation, the supernatant (900  $\mu$ L) from each aliquot was removed without disturbing the pellet. The pellet was resuspended in deionised water (800  $\mu$ L) and 4-MBA (100  $\mu$ L, 1 mM in EtOH) and left overnight. Unbound 4-MBA was removed *via* washing and centrifugation at 5500 rpm for 10 min. The supernatant (900  $\mu$ L) was removed without disturbing the pellet, followed by resuspension in dH<sub>2</sub>O (900  $\mu$ L). The samples were vortexed and sonicated to ensure the particles were forced back into suspension. The washing and centrifugation process was repeated a total of 3 times.

The functionalised nanoparticles were then concentrated and combined. The samples were centrifuged at 5500 rpm for 10 min, and the supernatant (950  $\mu$ L) was removed without disturbing the pellet. The AuNPs were forced back into suspension in the remaining volume of dH<sub>2</sub>O ( $\sim$ 50  $\mu$ L) through sonication and vortexing. The 5 aliquots were combined, centrifuged at 5500 rpm for 10 min, and the appropriate amount of supernatant was removed to give a final volume of 50  $\mu$ L.

**Fabrication of paper SERS substrate.** Preparation of the filter paper: an array of circular stencils was designed. A Xerox

ColourQube8580 was used to print in standard wax based ink on to the surface of the filter paper, leaving 3 mm diameter disks of bare paper. The wax printed paper was placed on a hotplate (150  $^{\circ}$ C) and compressed with a weight for 60s to ensure that the wax fully penetrated the paper.

For fabrication of the SERS-active substrate, 2  $\mu$ L droplets of the 4-MBA functionalised AuNPs were pipetted on to the filter paper disk and allowed to dry at room temperature for an hour. A further 6  $\mu$ L of AuNPs was dropped on to each disk in 2  $\mu$ L aliquots with drying in between to a total of 8  $\mu$ L ( $2.9 \times 10^9$  total particles deposited).

**Fibre sensing.** For preparation of the fibre-based sensor: silica based optical fibres (3  $\times$  1 m length, core diameter of 200  $\mu$ m, NA 0.39) were used throughout. The filter paper disks containing functionalised AuNPs had a 1 mm strip cut. The “top side” (the side of the filter paper to which AuNPs had been applied) was placed facing upwards on top of a rubber ring. A fibre ferrule was pushed through the ring resulting in the filter paper placed flush on the top of the ferrule. Following the preparation of the packaged ferrule, the fibre tip was threaded through to meet the filter paper and secured in place. A total of 3 fibres were prepared for calibration.

A SERS spectrum was obtained using the packaged distal end of the fibre from 7 separate pH buffers from pH 4–10. SERS spectra were acquired while the fibre tip was fully submerged in each buffer. Each of the 3 fibres were used for 3 replicate measurements between pH 4–10, with the order of the measurements within each replicate being random.

**Bacterial culture and extraction of *P. aeruginosa* 3284.** An inhouse clinical isolate *Pseudomonas aeruginosa* 3284 was used. A single colony was inoculated in Lysogeny Broth (LB; 10 mL) and incubated overnight (37  $^{\circ}$ C, 250 RPM), followed by a further subculture (100  $\mu$ L of overnight culture in 10 mL LB) and incubated at the same conditions for 4 hours until mid-log phase growth was reached.

The optical density at 595 nm (OD<sub>595</sub>) of the resulting culture was measured and adjusted to a value of 1 to give an approximate bacterial concentration of  $6 \times 10^8$  CFU mL<sup>-1</sup>. Serial dilutions ( $6 \times 10^8$  to  $6 \times 10^0$  CFU mL<sup>-1</sup>) were prepared with sterile PBS.

For each dilution, the packaged ferrule was dipped into the bacteria containing solution and pressed in succession across an LB agar plate. To compare, 3  $\times$  20  $\mu$ L samples of each dilution was dropped on lysogeny broth (LB) agar plates for CFU analysis. Plates were incubated at 37  $^{\circ}$ C with 5% CO<sub>2</sub> overnight, with CFUs manually counted.

After the paper ferrule had been pressed into LB agar, it was placed in an Eppendorf containing PBS (0.5 mL) and lightly vortexed. The paper and ferrule were removed and the bacteria containing solution labelled with a ubiquicidin-based probe (5  $\mu$ M), without a washing step. Immediately following the addition of the label, the solutions were placed in a confocal imaging chamber, pre-coated with poly-D-lysine (0.1 mg mL<sup>-1</sup>) and imaged by confocal laser scanning microscopy.

For direct imaging of bacteria on the paper, bacteria were first stained with Syto60 (5  $\mu$ M; Thermofisher), as per manu-





facturer's instructions, and washed twice with PBS by centrifugation at 13 000 rpm for 1 min. The AuNP paper was dipped into the stained bacterial solution containing  $6 \times 10^5$  CFUs per mL and imaged using widefield microscopy.

## Conclusions

In this study, a facile, inexpensive and reproducible paper-based SERS sensor has been integrated with optical fibre technology for use in pH sensing across a physiological relevant range. Using a patterned wax printed stencil to control the wicking boundary of AuNPs, the distribution of particles can be controlled across the paper. In addition, due to the wicking nature of the filter paper, it was possible to extract the bacteria, *P. aeruginosa*, demonstrating the dual-purpose ability of the paper substrate to acquire physiological and pathogenic information.

## Conflicts of interest

The authors have no conflicts to declare.

## Acknowledgements

This work was supported by the Engineering and Physical Sciences Research Council (EPSRC) and Medical Research Council (MRC) under grant number EP/L016559/1 (OPTIMA), and the School of Chemistry, University of Edinburgh; and the EPSRC Interdisciplinary Research Collaboration (EP/K03197X/1).

## References

- 1 J. O'Neill, *Tackling drug-resistant infections globally: final report and recommendations*, H M Government/Wellcome Trust, 2016.
- 2 S. Ramírez-Estrada, B. Borgatta and J. Rello, *Infect. Drug Resist.*, 2016, **9**, 7–18.
- 3 R. P. Baughman, D. A. Keeton, C. Perez and R. W. Wilmott, *Am. J. Respir. Crit. Care Med.*, 1997, **156**, 286–291.
- 4 H. Wang, X. Gu, Y. Weng, T. Xu, Z. Fu, W. Peng and W. Yu, *BMC Pulm. Med.*, 2015, **15**, 94.
- 5 J. R. Lentino and D. A. Lucks, *J. Clin. Microbiol.*, 1987, **25**, 758–762.
- 6 K. C. Carroll, *J. Clin. Microbiol.*, 2002, **40**, 3115–3120.
- 7 A. Zumla, J. A. Al-Tawfiq, V. I. Enne, M. Kidd, C. Drosten, J. Breuer, M. A. Muller, D. Hui, M. Maeurer, M. Bates, P. Mwaba, R. Al-Hakeem, G. Gray, P. Gautret, A. A. Al-Rabeeah, Z. A. Memish and V. Gant, *Lancet Infect. Dis.*, 2014, **14**, 1123–1135.
- 8 A. Dalhoff, S. Schubert and U. Ullmann, *Infection*, 2005, **33**, 36–43.
- 9 W. F. Walkenhorst, J. W. Klein, P. Vo and W. C. Wimley, *Antimicrob. Agents Chemother.*, 2013, **57**, 3312–3320.
- 10 A. Jaworska, L. E. Jamieson, K. Malek, C. J. Campbell, J. Choo, S. Chlopicki and M. Baranska, *Analyst*, 2015, **140**, 2321–2329.
- 11 L. E. Jamieson, V. L. Camus, P. O. Bagnaninchi, K. M. Fisher, G. D. Stewart, W. H. Nailon, D. B. McLaren, D. J. Harrison and C. J. Campbell, *Nanoscale*, 2016, **8**, 16710–16718.
- 12 D. Choudhury, M. G. Tanner, S. McAughtrie, F. Yu, B. Mills, T. R. Choudhary, S. Seth, T. H. Craven, J. M. Stone, I. K. Mati, C. J. Campbell, M. Bradley, C. K. I. Williams, K. Dhaliwal, T. A. Birks and R. R. Thomson, *Biomed. Opt. Express*, 2017, **8**, 243.
- 13 K. Ehrlich, A. Kufcsák, S. McAughtrie, H. Fleming, N. Krstajic, C. J. Campbell, R. K. Henderson, K. Dhaliwal, R. R. Thomson and M. G. Tanner, *Opt. Express*, 2017, **25**, 30976.
- 14 J. C. C. Day and N. Stone, *Appl. Spectrosc.*, 2013, **67**, 349–354.
- 15 R. P. Gandhiraman, D. Nordlund, V. Jayan, M. Meyyappan and J. E. Koehne, *ACS Appl. Mater. Interfaces*, 2014, **6**, 22751–22760.
- 16 E. P. Hoppmann, W. W. Yu and I. M. White, *Methods*, 2013, **63**, 219–224.
- 17 C. H. Lee, M. E. Hankus, L. Tian, P. M. Pellegrino and S. Singamaneni, *Anal. Chem.*, 2011, **83**, 8953–8958.
- 18 R. Derda, S. K. Y. Tang, A. Laromaine, B. Mosadegh, E. Hong, M. Mwangi, A. Mammoto, D. E. Ingber and G. M. Whitesides, *PLoS One*, 2011, **6**, 5.
- 19 D. A. Bruzewicz, M. Reches and G. M. Whitesides, *Anal. Chem.*, 2008, **80**, 3387–3392.
- 20 A. W. Martinez, S. T. Phillips, M. J. Butte and G. M. Whitesides, *Angew. Chem., Int. Ed.*, 2007, **46**, 1318–1320.
- 21 P. R. Stoddart and D. J. White, *Anal. Bioanal. Chem.*, 2009, **394**, 1761–1774.
- 22 G. F. S. Andrade, M. Fan and A. G. Brolo, *Biosens. Bioelectron.*, 2010, **25**, 2270–2275.
- 23 S. W. Bishnoi, C. J. Rozell, C. S. Levin, M. K. Gheith, B. R. Johnson, D. H. Johnson and N. J. Halas, *Nano Lett.*, 2006, **6**, 1687–1692.
- 24 F. Wang, R. G. Widejko, Z. Yang, K. T. Nguyen, H. Chen, L. P. Fernando, K. A. Christensen and J. N. Anker, *Anal. Chem.*, 2012, **84**, 8013–8019.
- 25 R. P. Dickson, J. R. Erb-Downward and G. B. Huffnagle, *Lancet Respir. Med.*, 2014, **2**, 238–246.
- 26 A.-P. Magiorakos, C. Suetens, D. L. Monnet, C. Gagliotti and O. E. Heuer, *Ant. Res. Infect. Control*, 2013, **2**, 6.
- 27 R. Lozano, M. Naghavi, K. Foreman, S. Lim, *et al.*, *Lancet*, 2012, **380**, 2095–2128.
- 28 J. Chastre and J.-Y. Fagon, *Am. J. Respir. Crit. Care Med.*, 2002, **165**, 867–903.
- 29 J. B. J. Scholte, H. A. van Dessel, C. F. M. Linssen, D. C. J. Bergmans, P. H. M. Savelkoul, P. M. H. J. Roekaerts and W. N. K. A. van Mook, *J. Clin. Microbiol.*, 2014, **52**, 3597–3604.



- 30 A. R. Akram, N. Avlonitis, A. Lilienkamp, A. M. Perez-Lopez, N. McDonald, S. V. Chankeshwara, E. Scholefield, C. Haslett, M. Bradley and K. Dhaliwal, *Chem. Sci.*, 2015, **6**, 6971–6979.
- 31 N. Krstajić, B. Mills, I. Murray, A. Marshall, D. Norberg, T. H. Craven, P. Emanuel, T. R. Choudhary, G. O. S. Williams, E. Scholefield, A. R. Akram, A. Davie, N. Hirani, A. Bruce, A. Moore, M. Bradley and K. Dhaliwal, *J. Biomed. Opt.*, 2018, **23**, 076005.
- 32 B. Mills, A. R. Akram, E. Scholefield, M. Bradley and K. Dhaliwal, *J. Visualized Exp.*, 2017, **129**, e56284.

